Title

Quantitative analysis of enteric neurons containing choline acetyltransferase and nitric oxide synthase immunoreactivities in the submucosal and myenteric plexuses of the porcine colon

Journal

Cell and Tissue Research, 383(2)

ISSN

0302-766X

Authors

Mazzoni, Maurizio
Caremoli, Filippo
Cabanillas, Luis
et al.

Publication Date

2021-02-01

DOI

10.1007/s00441-020-03286-7

Peer reviewed

HHS Public Access

Author manuscript

Cell Tissue Res. Author manuscript; available in PMC 2022 February 01.

Published in final edited form as:

Cell Tissue Res. 2021 February ; 383(2): 645–654. doi:10.1007/s00441-020-03286-7.

Quantitative analysis of enteric neurons containing choline acetyltransferase and nitric oxide synthase immunoreactivities in the submucosal and myenteric plexuses of the porcine colon

Maurizio Mazzoni[1,#], **Filippo Caremoli**[2,#], **Luis Cabanillas**[2], **Janira de los Santos**[3], **Mulugeta Million**[2,4], **Muriel Larauche**[2], **Paolo Clavenzani**[1], **Roberto De Giorgio**[5], **Catia Sternini**[2,3,*]

[1]Department of Veterinary Medical Sciences, University of Bologna, Ozzano Emilia, 40064 Bologna, Italy;

[2]Division of Digestive Diseases, Department Medicine, UCLA, Los Angeles, CA 90095, USA

[3]Department of Neurobiology, David Geffen School of Medicine, UCLA, Los Angeles, CA 90095, USA

[4]Department of Integrative Biology & Physiology, UCLA, Los Angeles, CA 90095, USA,

[5]Department of Medical Sciences, University of Ferrara, Nuovo Arcispedale S. Anna, Ferrara, Italy.

Abstract

The enteric nervous system (ENS) controls gastrointestinal functions. In large mammals' intestine, it comprises an inner (ISP) and outer (OSP) submucous plexus and a myenteric plexus (MP). This study quantifies enteric neurons in the ISP, OSP and MP of the pig ascending (AC) and descending colon (DC) using the HuC/D, choline acetyltransferase (ChAT) and neuronal nitric oxide synthase (nNOS) neuronal markers in wholemount preparations with multiple labeling immunofluorescence. We established that the ISP contains the highest number of HuC/D neurons/mm^2, which were more abundant in AC vs. DC, followed by OSP and MP with similar density in AC and DC. In the ISP, the density of ChAT immunoreactive (IR) neurons was very similar in AC and DC (31% and 35%), nNOS-IR neurons were less abundant in AC than DC (15% vs. 42%, $P< 0.001$) and ChAT/nNOS-IR neurons were 5% and 10%, respectively. In the OSP, 39–44% of neurons were ChAT-IR in AC and DC, while 45% and 38% were nNOS-IR and 10–12%

[*]**Corresponding author**: Catia Sternini, MD, Division of Digestive Diseases, David Geffen School of Medicine at UCLA, CHS 44-138, 650 Charles E. Young Dr. South, Los Angeles, CA 90095, USA csternin@ucla.edu.
[#]Mazzoni Maurizio and Filippo Caremoli contributed equally to the work.

Conflict of Interest

The authors declare that they have no conflict of interest.

Ethical approval

Animal care and procedures described in this study were carried out in strict accordance with the National Institutes of Health recommendations for the humane use of animals. The experimental procedures were approved by University of California, Los Angeles (UCLA), Chancellor's Animal Research Committee (ARC) (protocol 2018-074-01).

were ChAT/nNOS-IR (AC vs. DC $P < 0.05$). In the MP, ChAT-IR neurons were 44% in AC and 54% in DC ($P < 0.05$), nNOS-IR neurons were 50% in both and ChAT/nNOS-IR neurons were 12 and 18%, respectively. The ENS architecture with multilayered submucosal plexuses and the distribution of functionally distinct groups of neurons in the pig colon are similar to humans, supporting the suitability of the pig as a model and providing the platform for investigating the mechanisms underlying human colonic diseases.

Keywords

Enteric nervous system; excitatory motor neurons; inhibitory motor neurons; secretomotor neurons; interneurons

Introduction

The enteric nervous system (ENS) is embedded in the wall of the gastrointestinal (GI) tract, extends throughout its length and contains integrated circuits through which it regulates a variety of functions independently from the central nervous system (Furness 2012; Furness et al. 2014; Avetisyan et al. 2015). The structure of the ENS varies with the species and the region of the GI tract. In large mammals, including the pig, enteric neurons are grouped into three separate ganglionated plexuses, which are interconnected with a dense network of nerve processes (Timmermans et al. 1992). The myenteric plexus (MP) is located between the longitudinal and circular muscles; the outer submucous plexus (OSP) is immediately adjacent to the internal side of the circular muscle layer; and the inner submucous plexus (ISP) is found at the submucosal side of the *muscularis mucosa* (Petto et al. 2015). Enteric neurons differ in terms of morphology, functions, electrophysiological properties, and neurochemical coding, which refers to the combination of neurochemical messengers/transmitters/modulators that characterize functionally distinct populations of enteric neurons (Timmermans et al. 1990; Timmermans et al. 1992; Furness 2000). The ENS contributes to the regulation of GI motility, secretion, intestinal blood flow and ion transport (Timmermans et al. 1992; Timmermans et al. 1997). Although there are anatomical differences between the porcine and human colons such as the presence of centrifugal and centripetal coils in the pig, which are absent in humans (Barone 1997), the pig GI tract has been proposed as a model for medical research because of many homologies with humans. These include weight and organ similarity, physiology and disease progression, the availability of genomic, transcriptomic, proteomic tools, the application of effective cloning and transgenic technologies as well as the presence of stable cell lines (Lunney 2007; Bassols et al. 2014; Brown and Timmermans 2004). Pigs and humans are also colon fermenters, have similar colonic microbial composition (Miller et al. 1987; Pang et al. 2007) and their colons possess unique structures of tenia and sacculations (Kararli 1995).

The aim of our study was to provide a thorough evaluation of the density of enteric neurons visualized with the pan-neuronal marker HuC/D (Murphy et al. 2007) in the different plexuses of the pig colon specifically comparing the ascending and descending regions and the relative abundance of enteric neurons containing choline acetyltransferase (ChAT), a marker for acetylcholine, a major excitatory transmitter, and neuronal nitric oxide synthase

(nNOS), a marker for nitric oxide, a major inhibitory transmitter, which affect other neurons and effector cells, e.g., smooth muscle, epithelial, and enteroendocrine cells (Harrington et al. 2010; Sanders and Ward 2019). For this purpose, wholemount preparations were used in order to facilitate quantitative neuronal analysis with multiple labeling immunofluorescence, high-resolution confocal microscopy and Imaris software for quantification.

Material and Methods

Tissue preparation

Animal care and procedures described in this study were carried out in strict accordance with the National Institutes of Health recommendations for the humane use of animals. The experimental procedures were approved by University of California, Los Angeles (UCLA), Chancellor's Animal Research Committee (ARC) (protocol 2018-074-01), and all efforts were made to avoid suffering. Specimens were obtained from 12 hours fasted 15 male castrated Yucatan minipigs (seven month of age and 25–30 Kg of body weight). All animals were anaesthetized by intramuscular application of midazolam (1 mg/kg, cat # 067595, Covetrus, Dublin, OH), ketamine (15 mg/kg, cat # 068317, Covetrus, Dublin, OH) and meloxicam (0.3 mg/kg, #049755, Covetrus, Dublin, OH). These animals first underwent colonic motility analysis with manometry probes apposed on the serosa, then tissues were collected 5 hours post induction of anesthesia. The ascending colon (AC) in correspondence to the central flexure and descending colon (DC) (about 30 cm from the anus) were collected. We have compared these tissues to specimens collected immediately after induction of anesthesia and we have not seen differences in the total density of enteric neurons and the localization of different neuronal markers, thus providing assurance that this procedure did not affect neuronal distribution and neurochemical expression.

The samples were immersed in 0.01 M phosphate buffer saline (PBS, pH 7.0) containing the L-type calcium channel blocker, nicardipine (20 mM) for 15–40 min. The tissues were then opened along the mesenteric border, vigorously flushed out with PBS and pinned tightly on balsa wood, mucosal surface facing down. Specimens were subsequently fixed in 2% paraformaldehyde containing 0.2% picric acid in PBS at 4 °C overnight, removed from the balsa wood, washed (3 × 10 min) in dimethyl-sulfoxide (DMSO, Sigma-Aldrich), followed by washing in PBS (3 × 10 min) and stored at 4 °C in PBS containing sodium azide (0.1%). Whole mount preparations of the MP were obtained by separating the longitudinal muscle layer with attached the MP from the submucosa and mucosa using a dissecting microscope. The mucosa was removed from the submucosa and the submucosal layer was separated into the inner (ISP) and outer (OSP) parts of the submucosal plexus.

Immunohistochemistry

In order to establish the total number of neurons in each plexus and the distribution of subclasses of neurons, HuC/D, ChAT and nNOS primary antibodies were used (Table 1). Initial single labeling immunofluorescence experiments determined each individual antibody best dilution and incubation time. Wholemount preparations were incubated in 10% normal goat serum (NGS, Sigma Aldrich) in PBS containing 1% Triton-X100 and 1% BSA for 1 hour at room temperature (RT) to reduce nonspecific binding of the secondary antibodies

and to permeabilize the tissue to the antisera. All primary and secondary antibodies were diluted in PBS containing 1% Triton-X100 and 3% NGS. Tissues were then incubated at 4°C in a humid chamber for 2 days with the primary antibody (e.g. mouse anti-HuC/D), washed in PBS (3 × 10 min), and incubated for 3 hours at RT in a humid chamber in a solution containing the secondary antibody (e.g. goat anti-mouse Alexa Fluor® 594 or 405) (Table 1). For double and triple-labeling experiments, we used the sequential staining procedure (Ho et al. 2003), which has been shown to produce the best staining/background ratio. This procedure also allows the use of two mouse monoclonal antibodies in the same preparation. For double labeling, tissue was incubated with the first primary antibody (e.g. rabbit anti-ChAT), followed by goat anti-rabbit Alexa Fluor® 488, then incubated with the second primary antibody, e.g. mouse anti-HuC/D followed by goat anti-mouse Alexa Fluor® 594.

For triple labeling, tissue was incubated with the first primary antibody, rabbit anti-ChAT, followed by goat anti-rabbit Alexa Fluor® 488, then incubated with the second primary, mouse anti-nNOS, followed by goat anti-mouse Alexa Fluor® 594, finally incubated with the third primary antibody, mouse anti-HuC/D, followed by goat anti-mouse Alexa Fluor® 405. Tissues were washed several times with appropriate normal serum in between steps. Affinity-purified secondary antibodies were used in all the experiments. Tissue preparations were mounted on gelatin-coated slides with ProLongTM Gold antifade reagent (Invitrogen). We have validated the sequential staining with mouse anti-nNOS and mouse anti-HuC/D antibodies in a pilot study. First, we used the two anti-nNOS antibodies (raised in rabbit and mouse) either mixed together or applied sequentially and observed a perfect immunolabeling overlap in both neurons and nerve fibers (Electronic Supplementary Material, Fig. S1). Secondly, we used serial cryostat sections (9 μm) of the dorsal root ganglia (DRG), which allow the identification of the same neurons in consecutive sections, and processed the sections for immunohistochemistry using mouse anti-HuC/D and rabbit-nNOS combined or mouse anti-HuC/D followed by mouse anti-nNOS using the sequential staining method as described above. We observed the same immunolabeling pattern with either primary nNOS antibodies and with either approach (Electronic Supplementary Material, Fig. S2).

Specificity of primary antibodies

The specificity of the monoclonal antibodies to nNOS and HuC/D and of the polyclonal rabbit anti-ChAT antiserum has been previously tested (Murphy et al., 2007; Russo et al. 2013; Hens et al. 2000). The specificity of the rabbit nNOS antiserum is supported by the complete overlap of the staining obtained with this antiserum and the mouse monoclonal anti-nNOS antibody (Electronic Supplementary Material Fig. S1).

Quantitative analysis of ISP, OSP and MP neurons

Specimens were examined using Zeiss LSM 880 Fast-Airyscan confocal microscope and the Imaris software (Imaris for Neuroscientist) for quantification. We counted the total number of neurons immunoreactive (-IR) for the generalized neuronal marker HuC/D in 94 whole mount preparations (53 for the AC and 41 for the DC, which included 35 preparations of the ISP, 18 of the OSP and 41 of the MP). The number of HuC/D-IR neurons was expressed as number of neurons per mm^2 and number of neurons per ganglion. We also counted the

number of ganglia per area analyzed (analyzed ganglionated area range 0.14–0.34 mm^2). A collection of neurons was considered a ganglion (and therefore included in the quantitative assessment) when it showed a minimum of 10 HuC/D-IR neuronal cell bodies. Extra-ganglionic neurons were not counted. We then counted the number of ChAT-, nNOS- or ChAT/nNOS-IR neurons and expressed them as number per mm^2 and percentage of the total number of HuC/D-IR neurons. Data were expressed as means ± standard error of the mean (SEM). One-way and two-way ANOVA followed by Bonferroni post-test for multiple comparisons were used for statistical analysis ($P< 0.05$ for significance). The statistical software package Prism 8.3.0 (GraphPad Software, San Diego, CA) was used for these analyses.

Results

Neuronal Density and Organization of ISP, OSP and MP

In both AC and DC, the highest density of HuC/D neurons/mm^2 was observed in the ISP (1183±129 and 578±110, P<0.01) followed by the OSP (327±81 and 321±73), and the MP (223±43 and 270±33) (Fig. 1 a). There was significant difference between the number of neurons/mm^2 in the ISP vs. OSP (P<0.001 in AC and P<0.05 in DC) and vs. MP (P<0.001 in AC and P<0.01 in DC). Similarly, the number of neurons/ganglion (Fig. 1 b) was significantly higher in the ISP (129±6 and 119±10) vs. OSP (37±2 and 39±4) in both AC and DC (P<0.001 and P<0.01, respectively), and was significantly higher than the MP in the AC (62±7, P<0.01) but not the DC (98±14). By contrast, the MP had higher number of neurons/ganglion in the DC vs. the AC (P<0.05) (Fig. 1 b). The ISP displayed a denser network of ganglia compared to the OSP and MP in both AC and DC. Specifically, ISP showed 24±5 and 40±11 ganglia/area analyzed in AC and DC, respectively, whereas in the OSP the number of ganglia/area analyzed was 7±2 in AC and 7±1 in DC ($P< 0.01$, ISP vs. OSP in DC) and in the MP, it was 8±1 in AC and 20±5 in DC ($P< 0.05$, ISP vs. MP in DC) (Fig. 1 c).

The anti-HuC/D antibody, used for the evaluation of the neuronal populations, uniformly labeled the cytoplasm and often also the nucleus of virtually all neuronal cell bodies but not neuronal processes (Fig. 2 a, d, g). By contrast, nNOS and ChAT immunostaining visualized neuronal cell bodies and neuronal processes forming bundles separating the ganglia (Fig.2 b, e, h). Different morphological types of neurons were identified in submucosal and myenteric plexuses, including neurons with elongated cell bodies and thick dendrites (Fig. 2 b) and neurons with oval and smooth shape cell body and long, thick axons (Fig. 2 e, h).

ChAT and nNOS neurons

ChAT-IR neurons made up about a third of all neurons in the ISP of both AC and DC (35% ±2 and 31%±3) (Fig. 3 a, Fig. 4 b) and were more abundant in the OSP of both AC and DC (39%±7 and 44%±3). In the MP, ChAT-IR neurons were 44%±2 of all neurons in the AC (P<0.05 vs. ISP) and 54%±3 in the DC (P<0.001 vs. ISP) (Fig. 3 a, Fig. 5 b). nNOS-IR neurons were much less abundant in the ISP of AC than DC (15%±1 vs. 42%±4, P<0.001) (Fig. 3 b, Fig. 4 c), whereas there were no significant differences between nNOS-IR neurons in the OSP of AC and DC (45%±2 and 38%±1) or between nNOS-IR neurons in the MP of

AC and DC (50±4% and 50±5%) (Fig. 3 b, Fig. 5 c). There was a small population of neurons that co-expressed ChAT/nNOS-IR in the ISP (5%±1 in the AC and 10%±3 in the DC) (Fig. 3 d), whereas in the OSP, ChAT/nNOS-IR neurons were 10%±1 of enteric neurons in AC and 12%±3 in the DC (Fig. 3 c). In the MP, ChAT/nNOS-IR neurons were 12%±1 of the total number of myenteric neurons in the AC ($P<0.05$ vs. ISP) and 18%±2 in the DC ($P<0.05$ vs. ISP; $P<0.05$ vs. MP in AC; Fig. 3 c, Fig. 5 d).

Figures 4 and 5 show examples of HuC/D/ChAT-, HuC/D/nNOS- and HuC/D/ChAT/-nNOS-IR neurons in the ISP (Fig. 4) and the MP (Fig. 5). However, there are also HuC/D-IR neurons that do not contain ChAT- or nNOS-IR as shown in the ISP (Fig. 4) as well as in OSP and MP (not shown). Many ChAT/nNOS-IR neurons in the MP (Fig. 5) but also in the ISP show elongated cell bodies and thick dendrites, though it is more difficult to assess neuronal morphology in the ISP because of the density of enteric neurons.

Discussion

In the present study, we quantified the neurons in ascending and descending pig colon and compared their distribution and density in the submucosal and myenteric plexuses using the pan-neuronal marker anti-HuC/D (Barami et al. 1995), which is useful to assess the total number of neurons in the ENS (Murphy et al. 2007). We also used markers for two major transmitters, ChAT, the synthesizing enzyme for acetylcholine, and nNOS, the enzyme catalyzing the production of nitric oxide. Acetylcholine and nitric oxide are key transmitters mediating excitatory and inhibitory inputs, respectively, which are expressed in the vast majority of enteric neurons across species, including humans (Brookes 2001; Sang and Young 1998; Porter et al. 1996; 1997; Wattchow et al. 2008; Murphy et al. 2007; Harrington et al., 2010; Sanders and Ward 2019). This study shows differences in the density of the overall neuronal populations with the ISP displaying a dense network with a higher number of neurons/mm^2 compared to the OSP and MP in both AC and DC, and some differences in the abundance of ChAT-, nNOS- and ChAT/nNOS-IR neurons within plexuses and colonic segments that extend previous reports in this species and show similarities with findings in the human colon (Timmermans et al. 1990; Wedel et al. 1999; Wedel et al. 2002; Murphy et al., 2007; Wattchow et al., 2008; Petto et al. 2015 Ng et al., 2018).

Neurons containing ChAT-IR comprise functionally different classes of enteric neurons, including excitatory motor neurons, interneurons, primary afferent neurons and secretomotor neurons mostly based on studies in the guinea pig (Brookes 2001). Tracing studies in human colon showed that ChAT-IR in the MP project to the muscle layer supporting their motor neuron function (Wattchow et al., 1997; Porter et al. 1997; Brookes 2001; Porter et al. 2002). Similar types of studies in the pig small intestine indicate that a subset of ChAT-IR neurons in the ISP serve secretomotor function based on the projection of over 70% of them to the epithelium (Hens et al. 2000). Furthermore, electrophysiological studies provided evidence that acetylcholine released from cholinergic neurons evoked a strong prosecretory effect throughout the pig GI tract, including the colon (Chandan et al. 1991a, b; Leonhard-Marek et al. 2009; Pfannkuche et al. 2011). Moreover, ChAT-IR in the ISP and OSP colocalizes with substance P (unpublished; Petto et al., 2015), which acts as a secretagogue in the pig intestine (Brown at al., 1992; Pfannkuche et al. 2011). In addition, subpopulations of ChAT-

IR neurons in the ISP, OSP and MP likely serve as interneurons, since ChAT-IR fibers project within the ganglia in each plexus of the pig colon (Petto et al. 2015). Our findings of ChAT-IR in 44% and 54% of HuC/D-IR myenteric neurons in the AC and DC, respectively, are comparable to previous findings in human MP (Murphy et al., 2007, Ng et al., 2018, and Wattchow et al., 2008), confirming the high similarity between human and pig intestine. A previous study by Porter et al. (1996) reported a higher percentage of ChAT-IR neurons in human colon compared to our findings in the pig. However, this apparent discrepancy is likely attributable to the method used in the Porter (1996) study, which kept whole mount preparations in culture before processing for immunofluorescence to increase the ChAT immunostaining.

The role of nitric oxide in inhibitory transmission to the smooth muscle of the human intestine has been well established (Sanders and Ward 2019). The majority of nNOS-IR neurons are likely to function as inhibitory motor neurons and the high proportion of nNOS-IR motor neurons across species probably reflects a functional requirement for powerful inhibitory neuronal input to the muscle layers (Murphy et al. 2007). The density of nitrergic neurons found in our study in the MP (about 50%) is comparable to what described in the human colon (Murphy et al. 2007) and matches closely the numbers reported by Wattchow et al., (2008) in the AC and DC. The high abundance of nitrergic neurons in the OSP, which is much higher than in the ISP in the AC, is in accordance with previous findings in pig and human colon (Barbiers et al. 1993; Wester et al. 1998; Petto et al. 2015) and likely reflects an involvement in motility function given the close location of the OSP to the muscle layer. This is supported by the observation that nitrergic neurons of the OSP send processes to the circular muscle in both porcine and human intestine (Timmermans et al. 1994 a, b; Timmermans et al. 2001). Though we found that nNOS-IR are significantly less abundant in the ISP vs. OSP in the AC, the density of the nNOS-IR neurons in the ISP is much higher than previously reported in the piglet colon (Petto et al. 2015). Whether this discrepancy is due to the different age of the animals, 3 weeks old piglet (Petto et al. 2015) and adult pigs in our study cannot be excluded. Moreover, strain differences can contribute to different number of nNOS neurons as we investigated Yucatan minipigs, whereas Petto et al., (2015) used Landrace x Pietrain pigs. nNOS-IR fibers have been described in the porcine colonic mucosa (Pfannkuche et al. 2011) that are likely to derive from cell bodies in the submucosal plexuses, thus nNOS-IR neurons in the ISP and perhaps also the OSP might include secretomotor neurons.

The colocalization of ChAT- and nNOS-IR observed in our study in OSP and MP is consonant with previous findings in the piglet submucosal plexus (Petto et al. 2015) and in human myenteric neurons, respectively (Porter et al. 1997; Porter et al. 2002, Murphy et al. 2007). The ChAT/nNOS-IR neurons in the MP are likely descending interneurons as shown by tracing studies in the guinea pig and human colon suggesting conservation among species (Lomax and Furness 2000; Porter et al. 2002). In the pig ileum MP, ChAT/nNOS-IR neurons were also classified as descending interneurons (Brehmer et al. 2004). Furthermore, Porter et al. (2002) reported that ChAT and/or NOS antibodies labeled the majority of ascending and descending interneurons in the human colon and did not project to the circular muscle (Porter et al. 1997). However, ChAT/nNOS-IR neurons in the ISP and OSP are likely to also

include secretomotor neurons based on functional studies showing that acetylcholine and nitric oxide potentiate secretion in isolated epithelial cells (Pfannkuche et al. 2011).

In conclusion, our study provides a systematic and comprehensive analysis of neuronal density in each plexus in two distinct regions of the adult pig colon and the density and percentage of distinct populations of enteric neurons as identified by the expression and co-expression of two major transmitters using multiple immunofluorescence labeling and high resolution imaging. The pig submucosal plexus is multilayered as in human (Timmermans et al. 1990) and both the submucosal plexuses and the myenteric plexus contain $ChAT^{+}/nNOS^{-}$, $ChAT^{-}/nNOS^{+}$, $ChAT^{+}/nNOS^{+}$ and $ChAT^{-}/nNOS^{-}$ subpopulations as it has been reported in the human colon myenteric plexus (Porter et al. 2002; Murphy et al. 2007). Our findings in the adult pig ascending and descending colon expand the current knowledge of the pig intestine ENS, which mostly focused on the adult pig small intestine (Brehmer et al. 2004; Hens et al. 2000; Timmermans et al. 1990, 1994a, 1997), and the piglet large intestine (Petto et al., 2015). Our study further supports the proposal that the pig colon, despite the existence of some anatomical differences, is a valuable experimental model for translational research to explore pathophysiological mechanisms underlying colonic disorders in humans.

Supplementary Material

Refer to Web version on PubMed Central for supplementary material.

Acknowledgments and Funding

The present work was supported by National Institute of Health-SPARC (Stimulating Peripheral Activity to Relieve Conditions) Award 1OT2OD24899 (CS and MMillion); University of California at Los Angeles/Digestive Diseases Research Center Core P30 DK41301, Imaging Core (CS) and Animal Model Core (MMillion), and “Fondazione CARISBO” project 2017/0312, Bologna, Italy. The authors thank Prof. Michael Schemann for kindly providing the primary choline acetyl transferase antibody.

Funding

This study was funded by the National Institute of Health-SPARC (Stimulating Peripheral Activity to Relieve Conditions) Award 1OT2OD24899, the University of California at Los Angeles/Digestive Diseases Research Center Core P30 DK41301, and the “Fondazione CARISBO” project 2017/0312

References

Avetisyan M, Schill EM, Heuckeroth RO (2015) Building a second brain in the bowel. J Clin Invest 125:899–907 [PubMed: 25664848]

Barami K, Iversen K, Furneaux H, Goldman SA (1995) Hu protein as an early marker of neuronal phenotypic differentiation by subependymal zone cells of the adult songbird forebrain. J Neurobiol 28:82–101 [PubMed: 8586967]

Barbiers M, Timmermans J-P, Scheuermann DW, Adriaensen D, Mayer B, De Groodt-Lasseel MHA (1993) Distribution and morphological features of nitrergic neurons in the porcine large intestine. Histochemistry 100:27–34 [PubMed: 7693626]

Barone R (1997). Anatomie Comparée des Mammifères Domestiques. Splanchnologie I. Appareil Digestif, Appareil Respiratoire. Vigot Fréres Paris

Bassols A, Costa C, Eckersall PD, Osada J, Sabrià J, Tibau J (2014). The pig as an animal model for human pathologies: A proteomics perspective. Proteomics Clin Appl 8:715–731 [PubMed: 25092613]

Brehmer A, Schrodl F, Neuhuber W, Tooyama I, Kimura H (2004) Co-expression pattern of neuronal nitric oxide synthase and two variants of choline acetyltransferase in myenteric neurons of porcine ileum. J Chem Neuroanat 27:33–41 [PubMed: 15036361]

Brookes SJ (2001) Classes of enteric nerve cells in the guinea-pig small intestine. Anat Rec 262: 58–70 [PubMed: 11146429]

Brown DR, Parsons AM, O'Grady SM (1992) Substance P produces sodium and bicarbonate secretion in porcine jejunal mucosa through an action on enteric neurons. J Pharmacol Exp Ther 261:1206–1212. [PubMed: 1376357]

Brown DR, Timmermans JP (2004) Lessons from the porcine enteric nervous system. Neurogastroenterol Motil 16:50–54 [PubMed: 15066005]

Chandan R, Hildebrand KR, Seybold VS, Soldani G, Brown DR (1991a) Cholinergic neurons and muscarinic receptors regulate anion secretion in pig distal jejunum. Eur J Pharmacol 193:265–273 [PubMed: 2055245]

Chandan R, Megarry BH, O'Grady SM, Seybold VS, Brown DR (1991b) Muscarinic cholinergic regulation of electrogenic chloride secretion in porcine proximal jejunum. J Pharmacol Exp Ther 257:908–917 [PubMed: 2033527]

Furness JB (2000) Types of neurons in the enteric nervous system. J Auton Nerv Syst 81:87–96 [PubMed: 10869706]

Furness JB (2012) The enteric nervous system and neurogastroenterology. Nat Rev Gastroenterol Hepatol 9:286–94 [PubMed: 22392290]

Furness JB, Callaghan BP, Rivera LR, Cho HJ (2014) The enteric nervous system and gastrointestinal innervation: integrated local and central control. Adv Exp Med Biol 817:39–71 [PubMed: 24997029]

Hens J, Schrödl F, Brehmer A, Adriaensen D, Neuhuber W, Scheuermann DW, Schemann M, Timmermans JP (2000) Mucosal projections of enteric neurons in the porcine small intestine. J Comp Neurol 421:429–436 [PubMed: 10813797]

Harrington AM, Hutson JM, Southwell BR (2010) Cholinergic neurotransmission and muscarinic receptors in the enteric nervous system. Prog Histochem Cytochem 44:173–202 [PubMed: 20159236]

Ho A, Lievore A, Patierno S, Kohlmeier SE, Tonini M, Sternini C (2003) Neurochemically distinct classes of myenteric neurons express the μ-opioid receptor in the guinea pig ileum. J Comp Neurol 458:404–411 [PubMed: 12619074]

Kararli TT (1995) Comparison of the gastrointestinal anatomy, physiology, and biochemistry of humans and commonly used laboratory animals. Biopharm Drug Dispos 16:351–380 [PubMed: 8527686]

Leonhard-Marek S, Hempe J, Schroeder B, Breves G (2009) Electrophysiological characterization of chloride secretion across the jejunum and colon of pigs as affected by age and weaning. J Comp Physiol B 179:883–896 [PubMed: 19488761]

Lomax AE, Furness JB (2000) Neurochemical classification of enteric neurons in the guinea pig distal colon. Cell Tissue Res 302:59–78 [PubMed: 11079716]

Lunney JK (2007) Advances in swine biomedical model genomics. Int J Biol Sci 3:179–184 [PubMed: 17384736]

Miller ER, Ullrey DE (1987) The pig as a model for human nutrition. Annu Rev Nutr 7:361–382 [PubMed: 3300739]

Murphy EM, Defontgalland D, Costa M, Brookes SJ, Wattchow DA (2007) Quantification of subclasses of human colonic myenteric neurons by immunoreactivity to Hu, choline acetyltransferase and nitric oxide synthase. Neurogastroenterol Motil 19:126–134 [PubMed: 17244167]

Ng KS, Montes-Adrian NA, Mahns DA, Gladman MA (2018) Quantification and neurochemical coding of the myenteric plexus in humans: no regional variation between the distal colon and rectum. Neurogastroenterol Motil 30: doi: 10.1111/nmo.13193

Pang X, Hua X, Yang Q, Ding D, Che C, Cui L, Jia W, Bucheli P, Zhao L (2007) Inter-species transplantation of gut microbiota from human to pigs. ISME J 1:156–62 [PubMed: 18043625]

Petto C, Gäbel G, Pfannkuche H (2015) Architecture and chemical coding of the inner and outer submucous plexus in the colon of piglets. PLoS One 10:e0133350 [PubMed: 26230272]

Pfannkuche H, Mauksch A, Gabel G (2011) Modulation of electrogenic transport processes in the porcine proximal colon by enteric neurotransmitters. J Anim Physiol Anim Nutr (Berl) 96:482–93 [PubMed: 21623932]

Porter AJ, Wattchow DA, Brookes SJ, Schemann M, Costa M (1996) Choline acetyltransferase immunoreactivity in the human small and large intestine. Gastroenterology 111:401–8 [PubMed: 8690205]

Porter AJ, Wattchow DA, Brookes SJ, Costa M (1997) The neurochemical coding and projections of circular muscle motor neurons in the human colon. Gastroenterology 113:1916–1923 [PubMed: 9394731]

Porter AJ, Wattchow DA, Brookes SJ, Costa M (2002) Cholinergic and nitrergic interneurones in the myenteric plexus of the human colon. Gut 51:70–75 [PubMed: 12077095]

Russo D, Clavenzani P, Sorteni C, Bo Minelli L, Botti M, Gazza F, Panu R, Ragionieri L, Chiocchetti R (2013) Neurochemical features of boar lumbosacral dorsal root ganglion neurons and characterization of sensory neurons innervating the urinary bladder trigone. J Comp Neurol 521:342–66 [PubMed: 22740069]

Sanders KM, Ward SM (2019) Nitric oxide and its role as a non-adrenergic, non-cholinergic inhibitory neurotransmitter in the gastrointestinal tract. Br J Pharmacol 176:212–227 [PubMed: 30063800]

Sang Q, Young HM (1998) The identification and chemical coding of cholinergic neurons in the small and large intestine of the mouse. Anat Rec 251:185–199 [PubMed: 9624448]

Timmermans JP, Scheuermann DW, Stach W, Adriaensen D, De Groodt-Lasseel MH (1990) Distinct distribution of CGRP-, enkephalin-, galanin-, neuromedin U-, neuropeptide Y-, somatostatin-, substance P-, VIP- and serotonin-containing neurons in the two submucosal ganglionic neural networks of the porcine small intestine. Cell Tissue Res 260:367–379 [PubMed: 1694106]

Timmermans JP, Scheuermann DW, Stach W, Adriaensen D, de Groodt-Lesseal MHA (1992) Functional morphology of the enteric nervous system with special reference to large mammals. Eur J Morphol 30:113–122 [PubMed: 1457247]

Timmermans JP, Barbiers M, Scheuermann DW, Stach W, Adriaensen D, Mayer B, De Groodt-Lasseel MHA (1994a) Distributional pattern, neurochemical features and projections of nitrergic neurons in the pig small intestine. Ann Anat 176:515–525. [PubMed: 7530411]

Timmermans JP, Barbiers M, Scheuermann DW, Bogers JJ, Adriaensen D, Fekete E, Mayer B, Van Marck EA, De Groodt-Lasseel MHA (1994b) Nitric oxide synthase immunoreactivity in the enteric nervous system of the developing human digestive tract. Cell Tissue Res 275:235–245 [PubMed: 7509262]

Timmermans JP, Adriaensen D, Cornelissen W, Scheuermann DW (1997) Structural organization and neuropeptide distribution in the mammalian enteric nervous system, with special attention to those components involved in mucosal reflexes. Comp Biochem Physiol A Physiol 118:331–340 [PubMed: 9366065]

Timmermans JP, Hens J, Adriaensen D (2001) Outer submucous plexus: an intrinsic nerve network involved in both secretory and motility processes in the intestine of large mammals and humans. Anat Rec 262:71–78 [PubMed: 11146430]

Wattchow DA, Porter AJ, Brookes SJ, Costa M (1997) The polarity of neurochemically defined myenteric neurons in the human colon. Gastroenterology 113:497–506 [PubMed: 9247469]

Wattchow DA, Brookes S, Murphy E, Carbone S, de Fontgalland D, Costa M (2008) Regional variation in the neurochemical coding of the myenteric plexus of the human colon and changes in patients with slow transit constipation. Neurogastroenterol Motil 20:1298–1305 [PubMed: 18662329]

Wedel T, Roblick U, Gleiss J, Schiedeck T, Bruch HP, Kühnel W, Krammer HJ (1999) Organization of the enteric nervous system in the human colon demonstrated by wholemount immunohistochemistry with special reference to the submucous plexus. Ann Anat 181:327–337 [PubMed: 10427369]

Wedel T, Roblick UJ, Ott V, Eggers R, Schiedeck TH, Krammer HJ, Bruch HP (2002) Oligoneuronal hypoganglionosis in patients with idiopathic slow-transit constipation. Dis Colon Rectum 45:54–62 [PubMed: 11786765]

Wester T, O'Brian S, Puri P (1998) Morphometric aspects of the submucous plexus in wholemount preparations of normal human distal colon. J Pediatr Surg 33:619–622 [PubMed: 9574763]

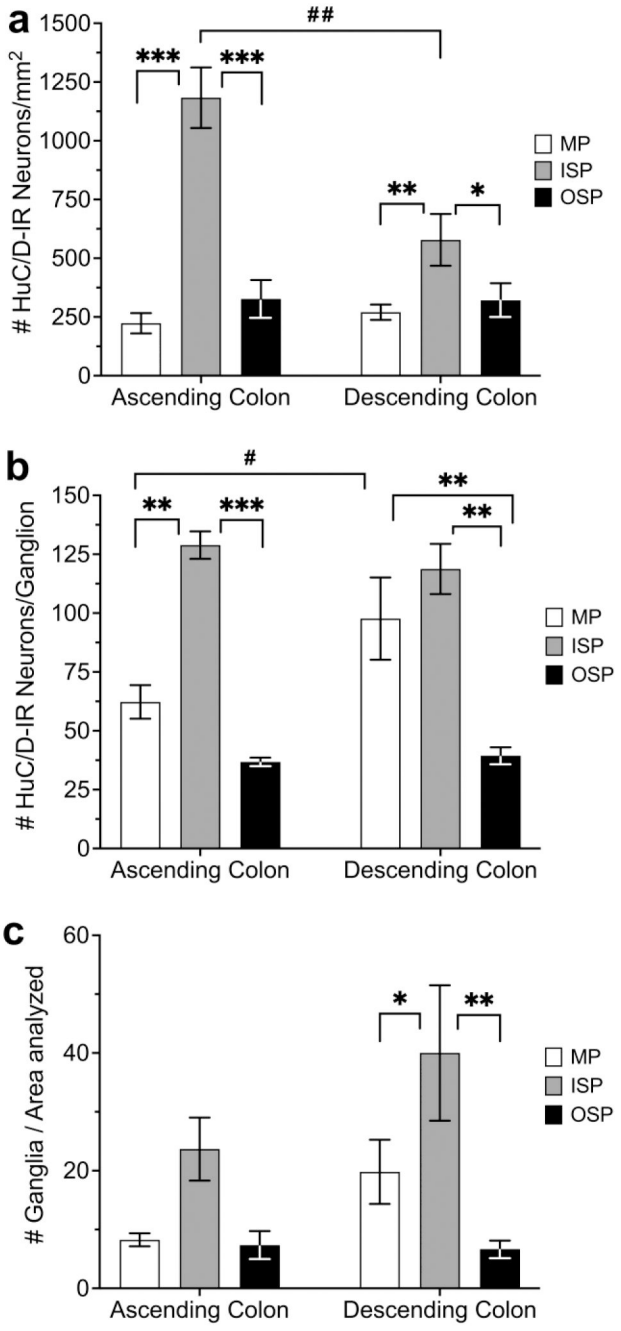

Fig. 1.

a-c Graphs showing the density of neurons visualized with the pan-neuronal marker HuC/D-immunoreactivity (IR) in the inner submucosal plexus (ISP), outer submucosal plexus (OSP) and myenteric plexus (MP) of the ascending and descending colon. Neuronal density is expressed as numbers of neurons/mm^2 **(a)** and numbers of neurons/ganglion **(b).** Graph in **(c)** shows the density of ISP, OSP and MP ganglia per area analyzed in the ascending and descending colon (* and # P<0.05; ** and ## P<0.01; *** P<0.001)

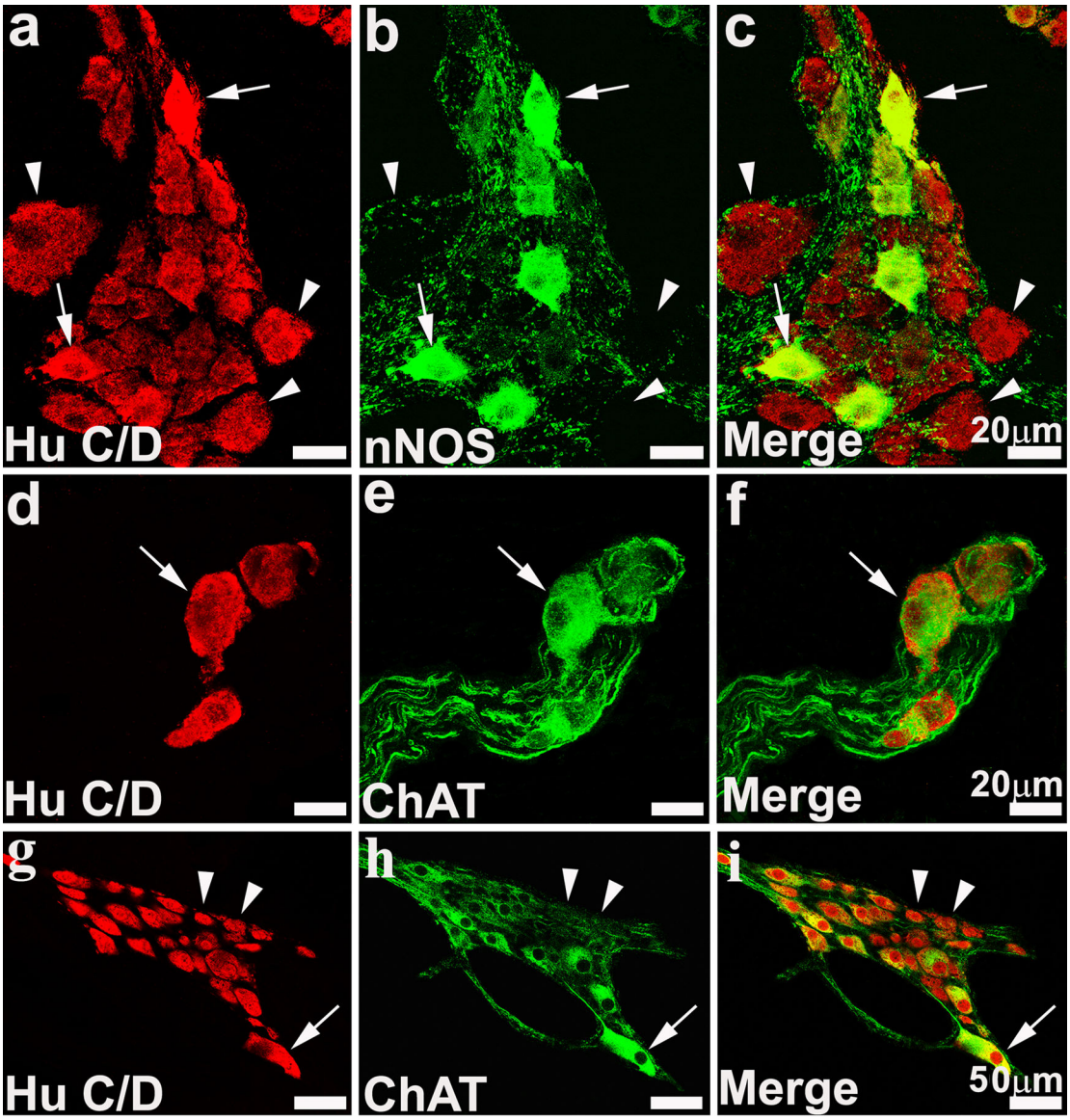

Fig. 2.

a-c High resolution confocal images of the inner submucosal plexus of the descending colon. **a.** Staining obtained with the pan-neuronal marker, HuC/D. **b.** nNOS immunoreactive (-IR) neurons (arrows) that exhibit an irregular, ovoidal soma profile with thick dendrites. Fibers in the ganglia show varicosities and make baskets around nNOS-negative neurons (arrowheads). **c.** Merge staining of HuC/D and nNOS. **d-f**. Outer submucosal plexus of the ascending colon. **d.** HuC/D-IR neurons, **e.** ChAT-IR neurons and **f**. merge staining. Arrows in **d-f** point to a neuron with a smooth and oval cell body with long filamentous (axon-dendritic) projections. **g-i.** Myenteric plexus of the ascending colon. Immunohistochemical co-localization of HuC/D **(g)** with ChAT-IR **(h)** and merge of the HuC/D- with ChAT-IR **(i)**. ChAT-IR neurons displayed a variable size and morphology. ChAT-IR was detectable in thinner and thicker bundles of fibers running around the HuC/D-IR neurons (arrowheads).

Arrow point to a ChAT-IR neuron with a prominent axon-dendritic projection and elongated smooth cell body

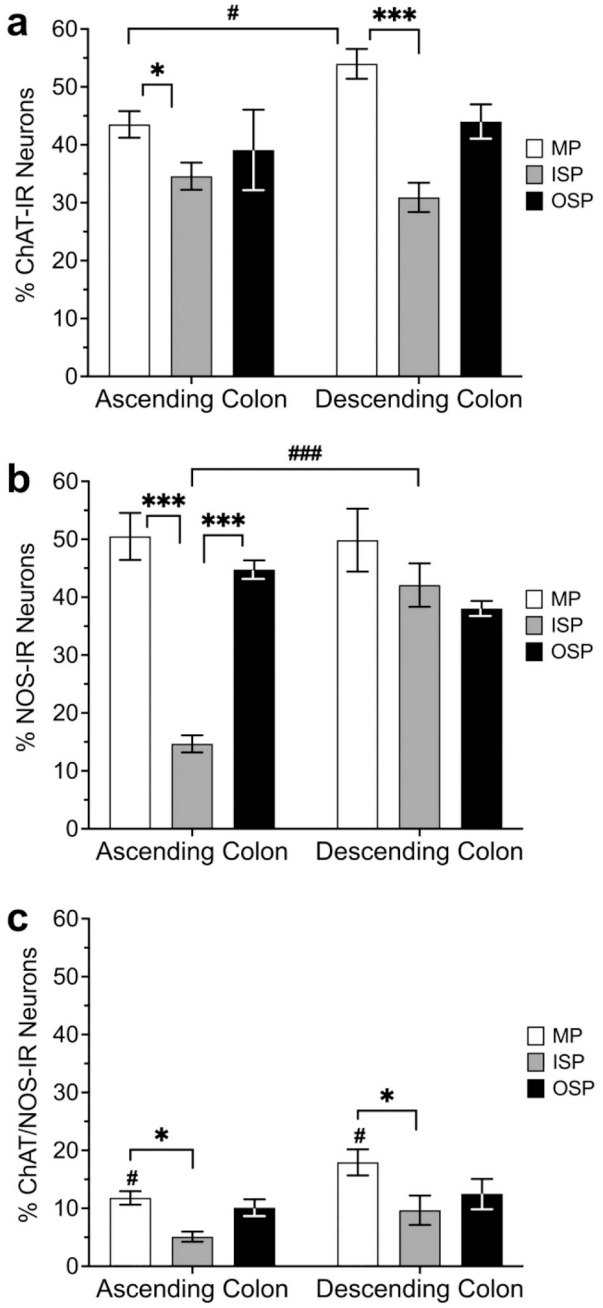

Fig. 3.

a, b, c Graphs showing the percentage of HuC/D-IR neurons expressing ChAT- (**a**), nNOS- **(b)** and ChAT/nNOS-IR **(c)** in the inner submucosal plexus (ISP), outer submucosal plexus (OSP) and myenteric plexus (MP) of the ascending and descending colon (* and #P<0.05 ***,###P<0.001).

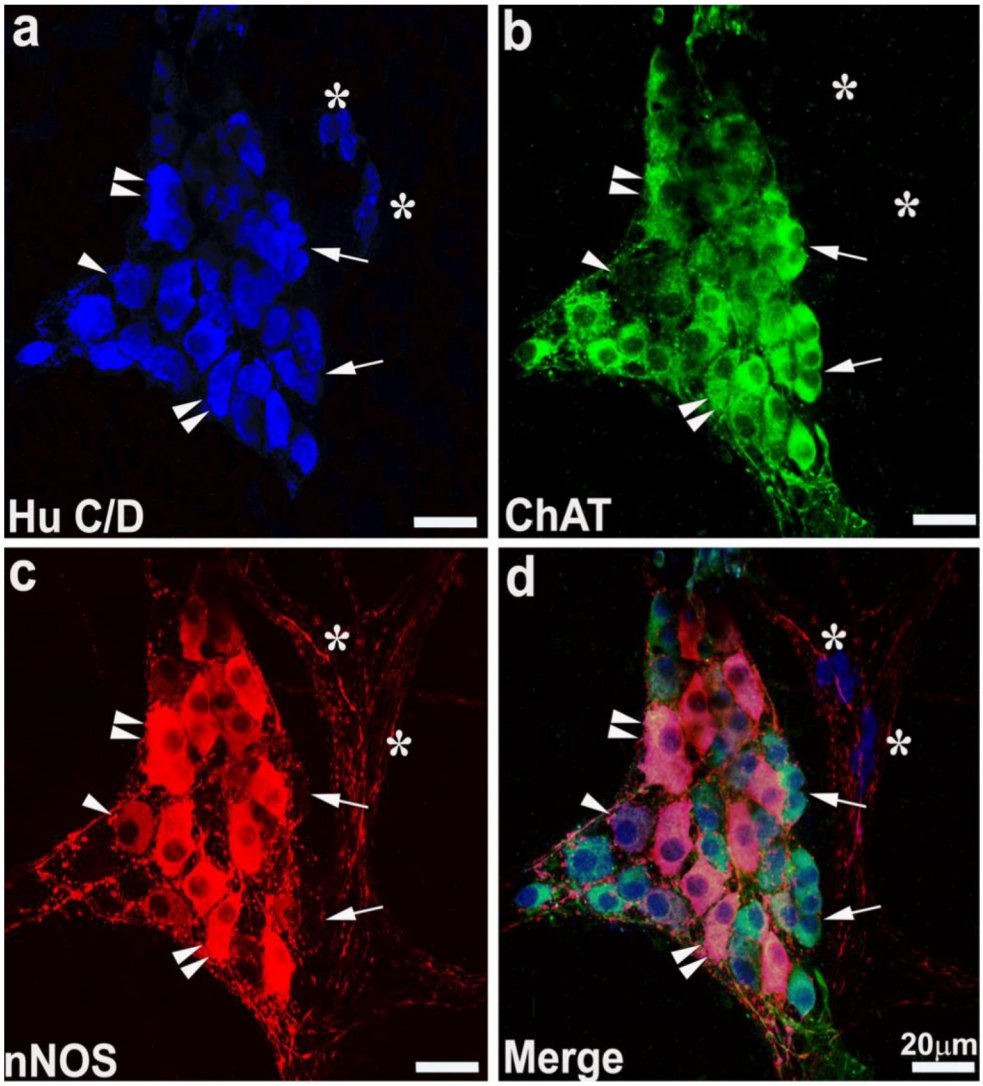

Fig. 4.

High resolution confocal images. Triple labeling of a ganglion in the inner submucosal plexus of the descending colon. The specimen was immunohistochemically stained for HuC/D (**a**), ChAT (**b**) and nNOS (**c**). (**d**) shows the overlay of the HuC/D, ChAT and nNOS-immunoreactivity (IR). Many HuC/D-IR neurons only contained ChAT-IR (arrows point to some representative examples). Arrowheads point to a HuC/D-IR neuron that is nNOS-IR but does not contain ChAT-IR and double arrowheads indicate HuC/D-IR neurons containing both ChAT- and nNOS-IR, whereas * indicate HuC/D-IR neurons negative for either ChAT- or nNOS-IR.

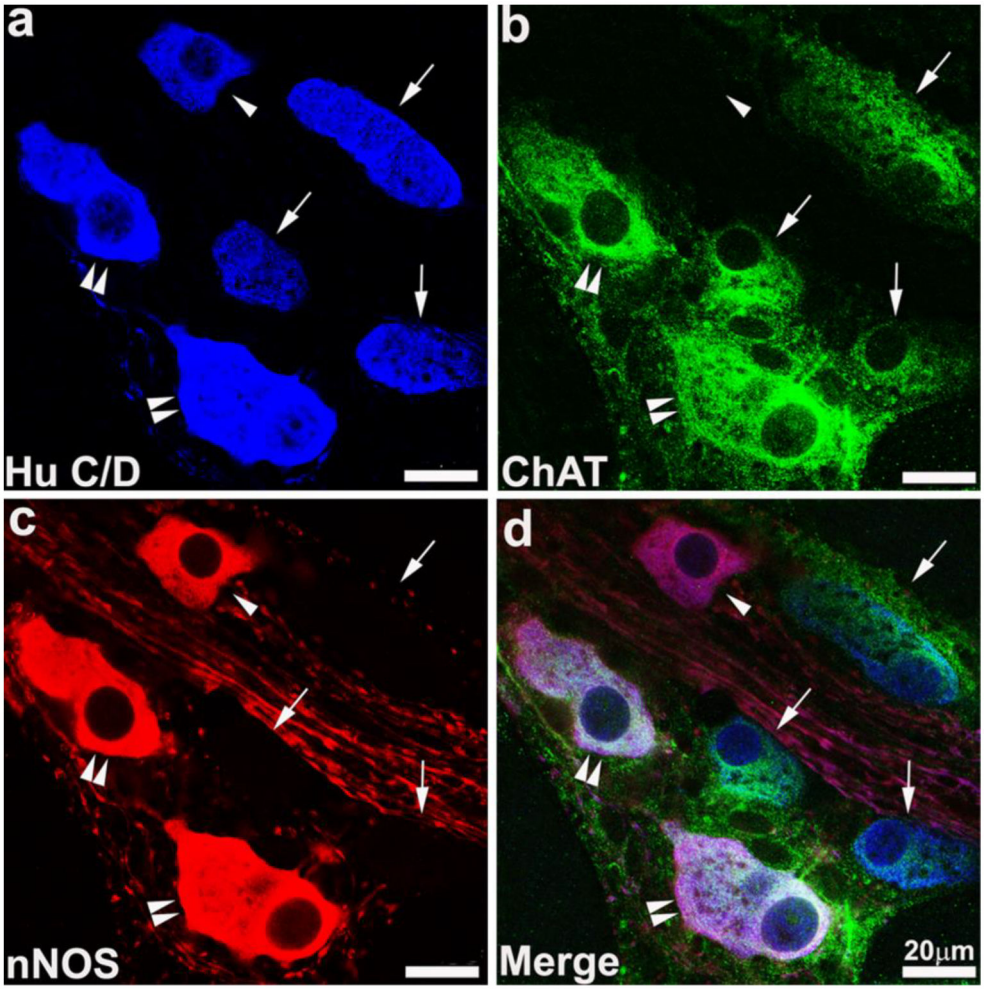

Fig. 5.

High resolution confocal images. Triple labeling of a ganglion in the myenteric plexus of the descending colon. The specimen was immunohistochemically stained for HuC/D (**a**), ChAT (**b**) and nNOS (**c**). **(d)** shows the overlay of HuC/D-, ChAT- and nNOS-IR. Arrows point to HuC/D-IR neurons containing ChAT-IR alone. Arrowheads point to HuC/D-IR neuron containing nNOS-IR but not ChAT-IR. Double arrowheads point to HuC/D-IR neurons containing ChAT- and nNOS-IR.

Table 1.

List of primary and secondary antibodies and their respective dilutions

Marker	Code	Case product	Dilutions
Mo anti-nNOS	SC-5302	Santa Cruz	1:100
Rb anti-nNOS	ab15203	Abcam	1:100
Rb anti-ChAT	P3YEB	(Prof. Schemann)	1:800
Mo anti-HuC/D	A-21271	Thermofisher Scientific	1:100
Secondary antibody			
Goat anti-mouse Alexa Fluor® 594	A11032	Thermofisher Scientific	1:800
Goat anti-rabbit Alexa Fluor® 488	A11008	Thermofisher Scientific	1:2000
Goat anti-mouse Alexa Fluor® 488	A11029	Thermofisher Scientific	1:1000
Goat anti mouse Alexa Fluor® 405	A31553	Thermofisher Scientific	1:1000